International Journal of Bifurcation and Chaos

IMPROVED HOMOCLINIC PREDICTOR FOR BOGDANOV-TAKENS BIFURCATION

YU.A. KUZNETSOV, H.G.E. MEIJER
Department of Applied Mathematics, University of Twente, Zilverling Building, P.O. Box 217, 7500AE Enschede, The Netherlands
[I.A.Kouznetsov, H.G.E.Meijer]@utwente.nl

B. AL HDAIBAT, W. GOVAERTS
Department of Applied Mathematics and Computer Science, Ghent University, Krijgslaan 281-S9, 9000 Gent, Belgium
[Bashir.AlHdaibat, Willy.Govaerts]@UGent.be

Received (to be inserted by publisher)

An improved homoclinic predictor at a generic codim 2 Bogdanov-Takens (BT) bifucation is derived. We use the classical "blow-up" technique to reduce the canonical smooth normal form near a generic BT bifurcation to a perturbed Hamiltonian system. With a simple perturbation method, we derive explicit first- and second-order corrections of the unperturbed homoclinic orbit and parameter value. To obtain the normal form on the center manifold, we apply the standard parameter-dependent center manifold reduction combined with the normalization, that is based on the Fredholm solvability of the homological equation. By systematically solving all linear systems appearing from the homological equation, we remove an ambiguity in the parameter transformation existing in the literature. The actual implementation of the improved predictor in MatCont and numerical examples illustrating its efficiency are discussed.

Keywords: Normal form, Bogdanov-Takens bifurcation, homoclinic orbit, center manifold, MatCont

1. Introduction

Equilibria with two zero eigenvalues can appear in generic smooth families of autonomous ODEs

$$\dot{x} = f(x, \alpha), \quad x \in \mathbb{R}^n, \alpha \in \mathbb{R}^m, \tag{1}$$

when $n \geq 2$ and $m \geq 2$. If the Jordan block

$$\begin{pmatrix} 0 & 1 \\ 0 & 0 \end{pmatrix}$$

is associated to these eigenvalues, such event is called a *Bogdanov-Takens* (BT) *bifurcation*. Bogdanov-Takens bifurcations of different codimensions play an important role in the analysis of dynamics of (1), since they imply the appearance of homoclinic orbits to saddle equilibria near the critical parameter values. These local homoclinic orbits are located in the 2D invariant center manifolds.

The exact bifurcation scenario near a BT-point is determined by an unfolding of the critical ODE on the 2D center manifold, with as many unfolding parameters as the codimension of the bifurcation. More

precisely, the bifurcation diagram of the unfolding depends on the coefficients of the critical normal form on the center manifold. The restriction of (1) to any center manifold at the critical parameter values can be transformed by formal smooth coordinate changes to the form

$$\begin{cases} \dot{w}_0 = w_1, \\ \dot{w}_1 = \sum\limits_{k\geq 2} \left(a_k w_0^k + b_k w_0^{k-1} w_1 \right) \end{cases} \tag{2}$$

(see, for example, [Arnold, 1983; Guckenheimer & Holmes, 1983]).

One of the most frequently used in applications bifurcations is the codim 2 BT with $a_2 b_2 \neq 0$, for which the complete bifurcation diagram for a generic two-parameter unfolding was obtained in 1970s [Takens, 1974; Bogdanov, 1975, 1976b,a]. The bifurcation diagram is presented in many textbooks (e.g., [Guckenheimer & Holmes, 1983; Kuznetsov, 2004]) and includes three bifurcation curves at which fold, Andronov-Hopf, and saddle-homoclinic bifurcations occur. The existence of the latter bifurcation curve makes this bifurcation particularly interesting, since it can be detected by the linear (eigenvalue) analysis but predicts a global (homoclinic) bifurcation for nearby parameter values.

There are standard methods to continue fold (limit point) and Hopf bifurcations of equilibria of ODEs in two parameters [Govaerts, 2000], as well as techniques for the two-parameter continuation of saddle homoclinic orbits given a suitable initial point [Champneys *et al.*, 1996; De Witte *et al.*, 2012]. One needs, therefore, a special predictor method to initialize the continuation of homoclinic solutions from a BT point. Since the homoclinic orbit shrinks to the equilibrium while tracing the homoclinic bifurcation curve, this predictor could be based on asymptotics for the bifurcation parameter values and the corresponding small homoclinic solutions in the phase space. Such asymptotics, i.e. a *homoclinic predictor*, were first derived by Beyn [1994]. Due to the existence of the parameter-dependent 2D center manifold near the bifurcation, the problem splits naturally into two sub-problems: (a) derive the asymptotics for the canonical normal form on the 2D center manifold; (b) transform the approximate homoclinic orbit into the phase- and parameter-space of a given generic n-dimensional ODE (1).

The general first step in solving sub-problem (a) is to perform a singular rescaling that brings the 2D normal form into a Hamiltonian system (with an explicit homoclinic solution) plus a small perturbation. Then one can use several methods to obtain an asymptotic expression for the parameter values corresponding to the perturbed homoclinic orbit. One possibility is to apply the classical Pontrayagin-Melnikov technique [Guckenheimer & Holmes, 1983] or equivalent branching methods [Beyn, 1994]. This technique easily provides the first-order approximation for the bifurcation parameter values in the perturbed Hamiltonian system, as well the zero-order approximation for the homoclinic orbit (i.e. the unperturbed Hamiltonian homoclinic loop). Obtaining higher-order approximations for the homoclinic solution with any of these methods is more involved and – according to our best knowledge – was never attempted before. The sub-problem (b) can either be solved with a Lyapunov-Schmidt method [Beyn, 1994], or using a parameter-dependent center manifold reduction combined with the normalization and based on the Fredholm solvability applied to the homological equation ([Beyn *et al.*, 2002] and below). However, all published solutions to this sub-problem are either incomplete or contain errors.

In the present paper, we revisit both sub-problems (in reversed order). For the sub-problem (a), we use the classical perturbation technique that allows us to derive a quadratic approximation to the homoclinic bifurcation curve and to obtain explicit first- and second-order corrections of the unperturbed homoclinic orbit. These corrections exhibit a counterintuitive behavior that will also be discussed. For the sub-problem (b), we systematically solve all linear systems appearing from the homological equation, thus removing an ambiguity in the parameter transformation present in [Beyn *et al.*, 2002]. By collecting all these results, we formulate an improved homoclinic predictor at a generic codim 2 BT bifucation. This new predictor is implemented in MatCont [Dhooge *et al.*, 2003, 2008] and proved to be more robust than the previous one based on [Beyn *et al.*, 2002].

The paper is organized as follows. In section 2, we describe the parameter-dependent center manifold reduction with normalization, which is an improved version of the method introduced in [Beyn *et al.*, 2002]. In section 3, we reduce the normal form to a perturbed Hamiltonian system and explicitly derive the first- and second-order approximations for the homoclinic solution. Section 4 combines the results obtained in the

previous sections and provides the explicit computational formulas for the improved homoclinic predictor. We present several numerical examples using an implementation in MatCont in Section 5.

2. Center manifold reduction combined with normalization

The predictor for homoclinic orbits emanating from equilibrium bifurcations is constructed within the framework of parameter-dependent center manifold reduction combined with normalization [Beyn *et al.*, 2002], that we briefly recall now.

2.1. *Method*

Suppose that system (1) has a codim 2 equilibrium $x = 0$ at $\alpha = 0$ and consider a normal form on the center manifold for this bifurcation

$$\dot{w} = G(w, \beta), \qquad G : \mathbb{R}^{n_c+2} \to \mathbb{R}^{n_c}. \tag{3}$$

Here $w \in \mathbb{R}^{n_c}$ parametrizes the n_c-dimensional parameter-dependent center manifold, while $\beta \in \mathbb{R}^2$ are the unfolding parameters. For all five codimension-2 equilibrium bifurcations these normal forms are well known (see, for example [Kuznetsov, 2004]). Suppose that an exact or approximate formula is available that gives an emanating codimension-1 bifurcation branch for the normal form (3). In order to transfer this to the original equation (1) we need a relation

$$\alpha = K(\beta), \qquad K : \mathbb{R}^2 \to \mathbb{R}^2 \tag{4}$$

between the unfolding parameters β and the original system parameters α and, moreover, we need a center manifold parametrization

$$x = H(w, \beta), \qquad H : \mathbb{R}^{n_c+2} \to \mathbb{R}^n. \tag{5}$$

Taking (4) and (5) together as $(x, \alpha) = (H(w, \beta), K(\beta))$ yields the center manifold for the suspended system $\dot{x} = f(x, \alpha), \dot{\alpha} = 0$. The invariance of the center manifold implies the *homological equation*

$$H_w(w, \beta)G(w, \beta) = f(H(w, \beta), K(\beta)), \tag{6}$$

which we can solve using Taylor series by a recursive procedure based on Fredholm's solvability condition that will give the Taylor coefficients with multi-index ν of G and H with respect to w and β. We write the Taylor expansion for f at $(x_0, \alpha_0) = (0, 0)$ as

$$\begin{aligned} f(x, \alpha) = {} & Ax + \tfrac{1}{2}B(x, x) \\ & + J_1\alpha + A_1(x, \alpha) + \tfrac{1}{2}J_2(\alpha, \alpha) \\ & + \mathcal{O}(\|x\|^3 + \|x\|\|\alpha\|^2 + \|x\|^2\|\alpha\| + \|\alpha\|^3), \end{aligned} \tag{7}$$

where $A = f_x(x_0, \alpha_0), J_1 = f_\alpha(x_0, \alpha_0)$, and B, A_1, and J_2 are the standard multilinear forms.

For $\nu = 0$ this procedure gives the critical normal form coefficients, while the coefficients with $|\nu| \geq 1$ yield the necessary data on the parameter dependence.

2.2. *Reduction near the BT-bifurcation*

Let $x_0 = 0,\ \alpha_0 = 0$ be a BT-point. Let q_0 and q_1 be real, linearly independent generalized eigenvectors of the Jacobian matrix $A = f_x(x_0, \alpha_0)$,

$$Aq_0 = 0, \quad Aq_1 = q_0,$$

and p_0 and p_1 be the corresponding eigenvectors of the transposed matrix A^T

$$A^T p_1 = 0, \quad A^T p_0 = p_1.$$

Using the standard inner product $\langle , \rangle$ we can assume that the vectors satisfy

$$\begin{aligned} \langle q_0, p_0 \rangle &= \langle q_1, p_1 \rangle = 1, \\ \langle q_1, p_0 \rangle &= \langle q_0, p_1 \rangle = 0. \end{aligned}$$

The smooth normal form for the BT bifurcation introduced in [Guckenheimer & Holmes, 1983] is

$$\begin{aligned}\dot{w} = G(w,\beta) = &\begin{pmatrix} w_1 \\ \beta_1 + \beta_2 w_1 + a w_0^2 + b w_0 w_1 \end{pmatrix} \\ &+ \mathcal{O}(\|w\|^3 + \|\beta\|\|w\|^2).\end{aligned} \tag{8}$$

This normal form is slightly different but equivalent to that used in [Bogdanov, 1976b,a], where the second unfolding term was $\beta_2 w_0$.

We use the homological equation (6) with the expansions

$$\begin{aligned}K(\beta) &= K_1\beta + \tfrac{1}{2}K_2\beta_2^2 \\ &\quad + \mathcal{O}(\beta_1^2 + |\beta_1\beta_2| + |\beta_2|^3) \\ H(w,\beta) &= H_{01}\beta + [q_0, q_1]w + \tfrac{1}{2}H_{20,0}w_0^2 \\ &\quad + H_{20,1}w_0w_1 + \tfrac{1}{2}H_{02,2}\beta_2^2 \\ &\quad + H_{21,0}\beta_1 w_0 + H_{21,1}\beta_1 w_1 \\ &\quad + H_{12,0}\beta_2 w_0 + H_{12,1}\beta_2 w_1 \\ &\quad + \mathcal{O}(|w_0|^3 + |w_0^2 w_1| + w_1^2) \\ &\quad + \mathcal{O}(\beta_1^2 + |\beta_1\beta_2| + |\beta_2|^3).\end{aligned} \tag{9}$$

From linear and quadratic w-terms in the homological equation, one obtains

$$\begin{aligned}a &= \tfrac{1}{2}p_1^T B(q_0, q_0), \\ b &= p_0^T B(q_0, q_0) + p_1^T B(q_0, q_1)\end{aligned} \tag{10}$$

(see, for example [Kuznetsov, 2004]). Moreover,

$$\begin{aligned}H_{20,0} &= A^{INV}(2aq_1 - B(q_0, q_0)), \\ H_{20,1} &= A^{INV}(bq_1 + H_{20,0} - B(q_0, q_1)).\end{aligned} \tag{11}$$

Using the expressions for a and b it is easily verified that the arguments of A^{INV} are in the range of A. In (11) we define $x = A^{INV}y$ by solving the non-singular bordered system

$$\begin{pmatrix} A & p_1 \\ q_0^T & 0 \end{pmatrix}\begin{pmatrix} x \\ s \end{pmatrix} = \begin{pmatrix} y \\ 0 \end{pmatrix}.$$

Collecting the linear β and $w\beta$-terms, the solvability condition applied to the resulting systems yields

$$AH_{01} + J_1K_1 = [q_1, 0], \tag{12}$$

$$\begin{aligned}&p_1^T B(q_0, H_{01}) + p_1^T A_1(q_0, K_1) \\ &\quad = \frac{1}{2}\left[p_1^T B(q_1, q_1), 0\right],\end{aligned} \tag{13}$$

$$\begin{aligned}&p_0^T B(q_0, H_{01}) + p_1^T B(q_1, H_{01}) \\ &\quad + p_0^T A_1(q_0, K_1) + p_1^T A_1(q_1, K_1) \\ &\quad = [-p_0^T B(q_1, q_1) + 3p_0^T H_{20,1}, 1].\end{aligned} \tag{14}$$

Taking (12), (13) and (14) together, one computes $K_1 = [K_{1,0}, K_{1,1}]$ and $H_{01} = [H_{01,0}, H_{01,1}]$ by solving the $(n+2)$-dimensional system

$$\begin{aligned}&\begin{pmatrix} A & J_1 \\ p_1^T \mathrm{B} q_0 & p_1^T A_1 q_0 \\ p_0^T \mathrm{B} q_0 + p_1^T \mathrm{B} q_1 & p_0^T A_1 q_0 + p_1^T A_1 q_1 \end{pmatrix}\begin{pmatrix} H_{01} \\ K_1 \end{pmatrix} \\ &\quad = \begin{pmatrix} q_1 & 0 \\ \frac{1}{2}p_1^T B(q_1, q_1) & 0 \\ -p_0^T B(q_1, q_1) + 3p_0^T H_{20,1} & 1 \end{pmatrix},\end{aligned} \tag{15}$$

where the expressions with matrix B have natural interpretation.

We note that the existence and uniqueness of the solution to (15) requires that the $(n+2)\times(n+2)$ matrix

$$M = \begin{pmatrix} A & J_1 \\ p_1^T \mathrm{B} q_0 & p_1^T A_1 q_0 \\ p_0^T \mathrm{B} q_0 + p_1^T \mathrm{B} q_1 & p_0^T A_1 q_0 + p_1^T A_1 q_1 \end{pmatrix} \tag{16}$$

is non-singular. The left $(n+2)\times n$ block has full rank n since the null vector q_0 of A is not orthogonal to the row vectors in the $(2,1)$ and $(3,1)$ block entries of M if $a \neq 0$ and $b \neq 0$. Since the right block column of M contains parameter derivatives in all entries, the non-singularity of M is the transversality condition for the BT point.

To prove that K_1 is non-singular we proceed by contradiction. Suppose that there exist real variables γ and η not both zero, such that $K_1 \begin{pmatrix}\gamma\\ \eta\end{pmatrix} = 0$. Then

$$M \begin{pmatrix}\xi\\0\\0\end{pmatrix} = \begin{pmatrix} \gamma q_1 \\ \frac{\gamma}{2} p_1^T B(q_1,q_1) \\ -\gamma p_0^T B(q_1,q_1) + 3\gamma p_0^T H_{20,1} + \eta \end{pmatrix}$$

with $\xi \in \mathbb{R}^n$. This implies that $A\xi = \gamma q_1$, hence $0 = p_1^T A\xi = \gamma p_1^T q_1 = \gamma$. Hence

$$M \begin{pmatrix}\xi\\0\\0\end{pmatrix} = \begin{pmatrix}0\\0\\\eta\end{pmatrix}$$

with $\eta \neq 0$. This, in turn, implies that $\xi = \mu q_0$ for a scalar $\mu \neq 0$. From the second block row in M we then have $\mu p_1^T B(q_0,q_0) = 0$, which contradicts $a \neq 0$.

The system (15) above corrects [Beyn, 1994; Beyn *et al.*, 2002], where a wrong formula to compute K_1 is suggested based on the assumption that K_1 satisfies the equation (12) only.

Finally, one finds the quadratic coefficients as in [Beyn *et al.*, 2002]

$$\begin{aligned} K_2 &= -(p_1^T z) K_{1,0}, \\ H_{02,2} &= -A^{INV}(z + J_1 K_2), \end{aligned} \tag{17}$$

where

$$\begin{aligned} z = {} & B(H_{01,1}, H_{01,1}) + 2A_1(H_{01,1}, K_{1,1}) \\ & + J_2(K_{1,1}, K_{1,1}), \end{aligned} \tag{18}$$

as well as

$$H_{12,0} = -A^{INV}(B(q_0, H_{01,1}) + A_1(q_0, K_{1,1})). \tag{19}$$

3. Homoclinic asymptotics in the 2D normal form

We consider now the problem of finding an explicit asymptotic for the homoclinic orbit in the BT normal form (8) for small parameter values.

The first step of the construction is a singular rescaling (blowup transformation) which anticipates the cuspoidal shape of the phase portrait in the (w_0, w_1)-plane. We truncate (8) at $\mathcal{O}(\|w\|^3 + \|w\|^2\|\beta\|)$, and apply a rescaling

$$\begin{aligned} & w_0 = \frac{\varepsilon^2}{a} u, \quad w_1 = \frac{\varepsilon^3}{a} v, \\ & \beta_1 = -\frac{4}{a}\varepsilon^4, \quad \beta_2 = \frac{b}{a}\varepsilon^2 \tau, \quad \varepsilon t = s. \end{aligned} \tag{20}$$

We obtain

$$\begin{cases} \dot{u} = v, \\ \dot{v} = -4 + u^2 + \varepsilon \frac{b}{a} v(\tau + u), \end{cases} \tag{21}$$

where the dot now indicates the derivative with respect to s. For $\varepsilon = 0$ the system is Hamiltonian.

The equilibria of (21) are the saddle $(2, 0)$ and the (degenerate) focus $(-2, 0)$ for sufficiently small $\varepsilon > 0$. The focus is stable if $ab > 0$, unstable if $ab < 0$. As noticed by Beyn [1994], a solution

$$\begin{pmatrix} u \\ v \\ \varepsilon \\ \tau \end{pmatrix} \in C^1(\mathbb{R}, \mathbb{R}) \times C^1(\mathbb{R}, \mathbb{R}) \times \mathbb{R} \times \mathbb{R}$$

to (21), where u and v are such that the limits

$$\lim_{s \to \pm\infty} \begin{pmatrix} u(s) \\ v(s) \end{pmatrix} \quad \text{and} \quad \lim_{s \to \pm\infty} \begin{pmatrix} \dot{u}(s) \\ \dot{v}(s) \end{pmatrix}$$

exist, defines a homoclinic orbit to the saddle $(2, 0)$ of (21) for the corresponding values of (ε, τ). Following Beyn[1994], we fix the phase of the homoclinic solutions by requiring that

$$v(0) = 0, \tag{22}$$

i.e. that the homoclinic orbit always crosses the u-axis at $s = 0$. For $\varepsilon = 0$ and any τ, the system (21) has the well-known homoclinic solution with $v_0(0) = 0$, namely

$$\begin{pmatrix} u_0(s) \\ v_0(s) \end{pmatrix} = 2 \begin{pmatrix} 1 - 3\mathrm{sech}^2(s) \\ 6\mathrm{sech}^2(s) \tanh(s) \end{pmatrix}. \tag{23}$$

Hence there exists a trivial branch $(u_0, v_0, 0, \tau)$ of homoclinic orbits in (21). It has been shown in [Beyn, 1994] that

$$\tau_0 = \frac{10}{7} \tag{24}$$

is a bifurcation point, at which a non-trivial smooth branch of homoclinic solutions of (21) emanates transversally. This branch can be parametrized by ε and approximated by

$$\begin{pmatrix} u \\ v \\ \varepsilon \\ \tau \end{pmatrix} = \sum_{l=0}^{L} \varepsilon^l \begin{pmatrix} u_l \\ v_l \\ 0 \\ \tau_l \end{pmatrix} + \varepsilon \begin{pmatrix} 0 \\ 0 \\ 1 \\ 0 \end{pmatrix}, \tag{25}$$

where the integer L defines the order of the approximation. Each (u_l, v_l) with $l \leq 1$ satisfies a linear inhomogeneous system that can be obtained by inserting the approximation into (21) and collecting the ε^l-terms for $l = 0, 1, 2, 3, \ldots$.

The ε^0-terms yield the Hamiltonian system, while the ε^1-terms yield

$$\begin{cases} \dot{u}_1 = v_1, \\ \dot{v}_1 = 2u_0u_1 + \frac{b}{a} v_0(\tau_0 + u_0). \end{cases} \tag{26}$$

A unique solution to (26) with $\lim_{s\to\pm\infty}(u_1(s), v_1(s)) = (0, 0)$ and satisfying $v_1(0) = 0$ will provide the first-order correction to the Hamiltonian homoclinic orbit, which Beyn [1994] was unable to find explicitly. In our case, it is possible since (26) has a simpler (normalized) form.

To obtain such a solution we first make the observation that $\varphi_1(s) = v_0(s)$ solves the homogeneous problem $\ddot{u}_1 = 2u_0u_1$. This enables us to find a second solution of the homogeneous problem by reducing it to a first order problem. This gives

$$\varphi_2(s) = 2\cosh^2(s) + 5 + \frac{15s\sinh(s)}{\cosh^3(s)} - \frac{15}{\cosh^2(s)}.$$

As we have two linearly independent solutions, it is now straightforward (although tedious) to solve the inhomogeneous problem $\ddot{u}_1 = 2u_0u_1 + \frac{b}{a} v_0(\tau_0 + u_0)$ with arbitrary τ_0. It is given by $u_1 = (c_1 - g)\varphi_1 + (c_2 + f)\varphi_2$

where c_1 and c_2 are yet undetermined integration constants and

$$\begin{aligned}
f(s) &= \frac{b}{35a}\frac{\sinh^3(s)(7\tau_0-10)}{\cosh^3(s)} \\
&\quad + \frac{3b}{70a}\frac{\sinh^3(s)(7\tau_0-10)}{\cosh^5(s)} - \frac{9b}{7a}\frac{\sinh^3(s)}{\cosh^7(s)}, \\
g(s) &= \frac{6b}{7a}\log(2\cosh(s)) + s\frac{b}{28a}\frac{\sinh(s)(7\tau_0-10)}{\cosh(s)} \\
&\quad + \frac{b}{28a}\frac{(-7\tau_0+1)}{\cosh^2(s)} + s\frac{b}{56a}\frac{\sinh(s)(7\tau_0-10)}{\cosh^3(s)} \\
&\quad + \frac{3b}{56a}\frac{(7\tau_0+30)}{\cosh^4(s)} + s\frac{3b}{56a}\frac{\sinh(s)(-7\tau_0-20)}{\cosh^5(s)} \\
&\quad - \frac{45b}{28a}\left(\frac{1}{\cosh^6(s)} - s\frac{\sinh(s)}{\cosh^7(s)}\right) \\
&\quad - \frac{b}{a}\left(\frac{\tau_0}{8} + \frac{1}{28} + \frac{6}{7}\log 2\right),
\end{aligned}$$

for which $f(0) = g(0) = 0$ holds. Now we check the limits of $u_1(s)$ for $s \to \pm\infty$. First we see that $\lim_{s\to\pm\infty} g(s)\varphi_1(s) = \lim_{s\to\pm\infty} \varphi_1(s) = 0$. So we focus on the other terms. We find $\lim_{s\to\pm\infty}(c_2 + f(s)) = c_2 \pm \frac{b}{a}\frac{7\tau_0-10}{35}$. Thus we recover $\tau_0 = \frac{10}{7}$ together with $c_2 = 0$. The phase condition $v_1(0) = 0$ gives $c_1 = 0$, so that

$$\begin{aligned}
u_1(s) &= -\frac{72b}{7a}\frac{\sinh(s)\log(\cosh(s))}{\cosh^3(s)}, \\
v_1(s) &= -\frac{72b}{7a}\frac{\sinh^2(s) + (1-2\sinh^2(s))\log(\cosh(s))}{\cosh^4(s)}.
\end{aligned} \tag{27}$$

Collecting the ε^2-terms leads to the linear inhomogeneous system

$$\begin{cases} \dot{u}_2 = v_2, \\ \dot{v}_2 = 2u_0u_2 + \frac{b}{a}v_0(\tau_1+u_1) + \frac{b}{a}v_1(\tau_0+u_0) + u_1^2, \end{cases} \tag{28}$$

where the homogeneous part has the same form as in (26). Thus, the general solution to (28) can be written as $u_2 = (c_3 - g_1)\varphi_1 + (c_4 + f_1)\varphi_2$ and $v_2 = \dot{u}_2$, where c_3 and c_4 are new integration constants, while g_1 and f_1 are certain functions satisfying $f_1(0) = g_1(0) = 0$, which we have obtained explicitly but are too long to be displayed here. A unique solution to (28) with $\lim_{s\to\pm\infty}(u_2(s), v_2(s)) = (0,0)$ and satisfying $v_2(0) = 0$ will provide the second-order correction to the Hamiltonian homoclinic orbit. The requirements $\lim_{s\to\pm\infty}(c_4 + f_1(s)) = 0$ imply $c_4 = \frac{9b^2}{196a^2}$ and $\tau_1 = 0$, while the phase condition $v_2(0) = 0$ gives $c_3 = 0$. The condition $\tau_1 = 0$ is equivalent to $\tau'(0) = 0$ established in [Beyn, 1994] using symmetry arguments.

At this point we can conclude that the *tangent line* to the homoclinic branch at the bifurcation point is given by

$$\begin{pmatrix} u \\ v \\ \varepsilon \\ \tau \end{pmatrix} = \begin{pmatrix} u_0 \\ v_0 \\ 0 \\ \tau_0 \end{pmatrix} + \varepsilon \begin{pmatrix} u_1 \\ v_1 \\ 1 \\ 0 \end{pmatrix}. \tag{29}$$

In Fig. 1(a) we have plotted the corresponding tangent predictor in the (u, v)-plane for several values of ε. It is remarkable, see also the close-up, that the orbits for $\varepsilon \neq 0$ approach the saddle along the "wrong" direction, making a "parasitic turn" when $s \to +\infty$ or $s \to -\infty$ (see Fig.1(b)). Indeed, the difference $2 - (u_0(s) + \varepsilon u_1(s))$ asymptotically behaves for $s \to \pm\infty$ as

$$\frac{288}{7}\frac{b}{a}\varepsilon s e^{\mp 2s},$$

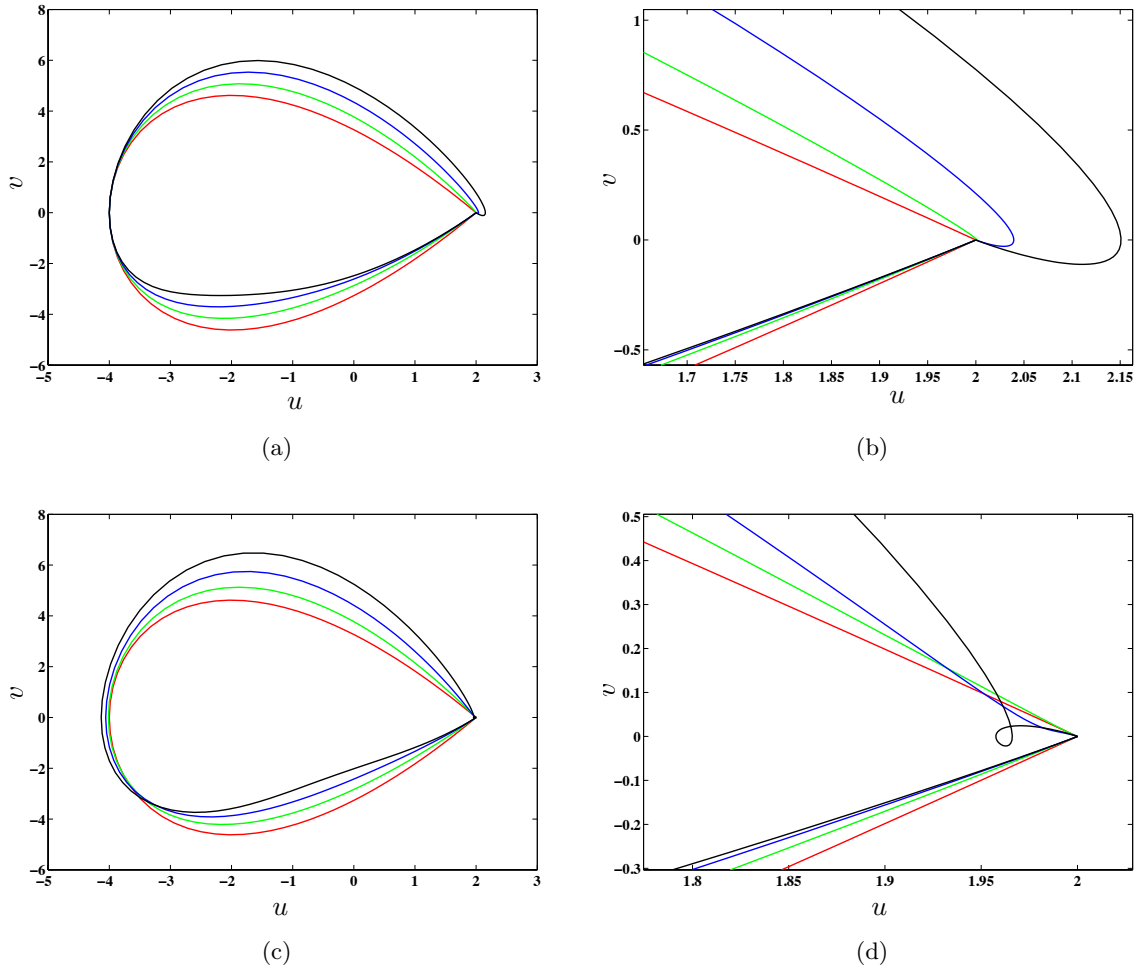

Fig. 1: Homoclinic orbit predictors for $(a, b) = (-1, 1)$ and $\varepsilon = 0$ (red), 0.2 (green), 0.4 (blue), 0.6 (black). (a) Tangent predictors; (b) Zoom of the tangent predictors near the saddle: the "parasitic turn" is clearly visible; (c) The second-order predictors; (d) Zoom of the second-order predictors near the saddle: the "parasitic loop" is present only for large ε.

and, therefore, is negative for $s \to -\infty$ if $ab > 0$ or for $s \to +\infty$ if $ab < 0$ (provided that $\varepsilon > 0$). When $\varepsilon \to 0$, this parasitic turn vanishes and on any finite time interval $[-T, T]$ the tangent predictor with sufficiently small ε does approximate the "true" homoclinic solution better than the Hamiltonian predictor with $\varepsilon = 0$. In particular, while the Hamiltonian homoclinic orbit (23) is symmetric w.r.t. the u-axis, the tangent predictor defines a non-symmetric approximate orbit, better corresponding to the non-symmetric true homoclinic orbit in (21) and in the normal form (8), see Section 5.1 for a graphical illustration.

With the found above constants c_3, c_4, and τ_1, one obtains

$$\begin{aligned}
u_2 &= -\frac{216b^2}{49a^2}\frac{\log^2(\cosh(t))(\cosh(2t)-2)}{\cosh^4(t)} \\
&\quad -\frac{216b^2}{49a^2}\frac{\log(\cosh(t))(1-\cosh(2t))}{\cosh^4(t)} \\
&\quad -\frac{18b^2}{49a^2}\frac{(6t\sinh(2t)-7\cosh(2t)+8)}{\cosh^4(t)}, \\
v_2 &= \frac{216b^2}{49a^2}\frac{t(2\cosh^2(t)-3)}{\cosh^4(t))} \\
&\quad +\frac{288b^2}{49a^2}\frac{\sinh(t)(3\log^2(\cosh(t))-6\log(\cosh(t)))}{\cosh^3(t)} \\
&\quad -\frac{216b^2}{49a^2}\frac{\sinh(t)(12\log^2(\cosh(t))-14\log(\cosh(t)))}{\cosh^5(t)} \\
&\quad -\frac{288b^2}{49a^2}\frac{\sinh(t)}{\cosh^3(t)}+\frac{648b^2}{49a^2}\frac{\sinh(t)}{\cosh^5(t)}.
\end{aligned}$$

Figs. 1(c) and (d) show the second-order predictor in the (u, v)-plane. While no "parasitic turn" exists for small ε, a "parasitic loop" appears for big values of ε. Thus implies that in actual computations ε must be small, as one naturally expects for asymptotic expansions.

Since we need the value of τ_2 in the next section, we have to make one more step. Collecting the ε^3-terms leads to the linear inhomogeneous system

$$\begin{cases} \dot{u}_3 = v_3, \\ \dot{v}_3 = 2u_0u_3 + \frac{b}{a}v_0(\tau_2+u_2) + \frac{b}{a}v_1(\tau_2+u_2) \\ \quad\quad + \frac{b}{a}v_2(\tau_0+u_0) + 2u_1u_2, \end{cases} \tag{30}$$

As before, $u_3 = (c_5 - g_2)\varphi_1 + (c_6 + f_2)\varphi_2$ for some functions g_2 and f_2 satisfying $f_2(0) = g_2(0) = 0$. The conditions $\lim_{s\to\pm\infty} u_3(s) = 0$ imply, in particular,

$$\tau_2 = \frac{288b^2}{2401a^2}. \tag{31}$$

Thus, the second-order approximation for the emanating homoclinic orbits for the BT normal form (8) is given by

$$\begin{aligned}
w_0(t) &= \frac{\varepsilon^2}{a}\left(u_0(\varepsilon t) + \varepsilon u_1(\varepsilon t) + \varepsilon^2 u_2(\varepsilon t)\right) \\
&\quad + \mathcal{O}(\varepsilon^5), \\
w_1(t) &= \frac{\varepsilon^3}{a}\left(v_0(\varepsilon t) + \varepsilon v_1(\varepsilon t) + \varepsilon^2 v_2(\varepsilon t)\right) \\
&\quad + \mathcal{O}(\varepsilon^6), \\
\beta_1 &= -\varepsilon^4\left(\frac{4}{a}\right) + \mathcal{O}(\varepsilon^5), \\
\beta_2 &= \varepsilon^2\tau_0\left(\frac{b}{a}\right) + \varepsilon^4\tau_2\left(\frac{b}{a}\right) + \mathcal{O}(\varepsilon^5),
\end{aligned} \tag{32}$$

where all ingredients are defined above.

4. Computational formulas for n-dimensional systems

In this section we provide an asymptotic expression for the bifurcating homoclinic solution of (1). To find the prediction, we transfer system (8) with our homoclinic approximation (32) back to the original form

(1). With data collected in (10) and (11), and using (15) and (17)-(19), we get the second-order homoclinic predictor for the original system (1)

$$\begin{aligned}\alpha &= \varepsilon^2 \frac{10b}{7a} K_{1,1} \\ &+ \varepsilon^4 \left(-\frac{4}{a} K_{1,0} + \frac{50b^2}{49a^2} K_2 + \frac{288b^3}{2401a^3} K_{1,1} \right) \\ &+ \mathcal{O}(\varepsilon^5)\end{aligned} \tag{33}$$

and

$$\begin{aligned}x(t) &= \varepsilon^2 \left(\frac{10b}{7a} H_{01,1} + \frac{1}{a} u_0(\varepsilon t) q_0 \right) \\ &+ \varepsilon^3 \left(\frac{1}{a} v_0(\varepsilon t) q_1 + \frac{1}{a} u_1(\varepsilon t) q_0 \right) \\ &+ \varepsilon^4 \left(-\frac{4}{a} H_{01,0} + \frac{50b^2}{49a^2} H_{02,2} + \frac{288b^3}{2401a^3} H_{01,1} \right. \\ &\quad + \frac{1}{a} u_2(\varepsilon t) q_0 + \frac{1}{a} v_1(\varepsilon t) q_1 \\ &\quad \left. + \frac{1}{2a^2} H_{20,0} u_0(\varepsilon t)^2 + \frac{10b}{7a^2} H_{12,0} u_0(\varepsilon t) \right) \\ &+ \mathcal{O}(\varepsilon^5).\end{aligned} \tag{34}$$

We note that the phase condition (22) could be replaced by a different one. We can fix the phase using an integral condition as in [Doedel & Kernévez, 1986; Champneys *et al.*, 1996] and [De Witte *et al.*, 2012]. Namely, we can fix the phase of $u(s)$ by requiring its minimal L_2-distance to the Hamiltonian approximation $u_0(s)$. Mathematically, this leads to $\int_{-\infty}^{+\infty} \langle u(s) - u_0(s), \dot{u}_0(s) \rangle ds = 0$ where $\dot{u}_0(s) = v_0(s)$. Applied for u_1 and u_2 separately, this gives different values of c_1 and c_4. However, extensive numerical tests did not show any substantial superiority of this choice over the predictor based on (33) and (34).

5. Examples

5.1. *Truncated normal form*

Consider the two-parameter system

$$\begin{cases} \dot{w}_0 = w_1, \\ \dot{w}_1 = \beta_1 + \beta_2 w_1 + a w_0^2 + b w_0 w_1, \end{cases} \tag{35}$$

that is the truncated normal form (8). Bifurcation analysis of this system has been presented, for example, in [Guckenheimer & Holmes, 1983]. In this system we have two equilibria $\left(\pm\sqrt{-\frac{1}{a}\beta_1}, 0 \right)$, which lie on the folded surface $S = \{(w_0, w_1, \beta_1, \beta_2) = (s, 0, -as^2, \beta_2) : s, \beta_2 \in \mathbb{R}\}$. We want to compare the predicted homoclinic solution with that obtained via the high-accuracy numerical continuation in MatCont [De Witte *et al.*, 2012].

Substituting $\tau = \tau_0 + \tau_2 \varepsilon^2$ with (24) and (31) into (20), we obtain the following second-order approximation for the homoclinic bifurcation curve in the parameter plane (β_1, β_2) of (35):

$$\beta_2 = -\frac{72b^3}{2401a^2} \beta_1 + \frac{5b}{7a} \sqrt{-a\beta_1} \tag{36}$$

for $\text{sign}(\beta_1) = -\text{sign}(a)$. For $a = -1$ and $b = 1$, this approximation is shown as the red curve Hom^{Pred} in Fig.2a.

We use MatCont to start a continuation of equilibria with initial parameter values $(\beta_1,\, \beta_2) = (1, -2)$ and the equilibrium point $(w_0, w_1) = (1, 0)$; β_2 is the free parameter. Two bifurcation points are detected along the curve of equilibria, limit point (LP) and Hopf (H). The LP continuation is now carried out

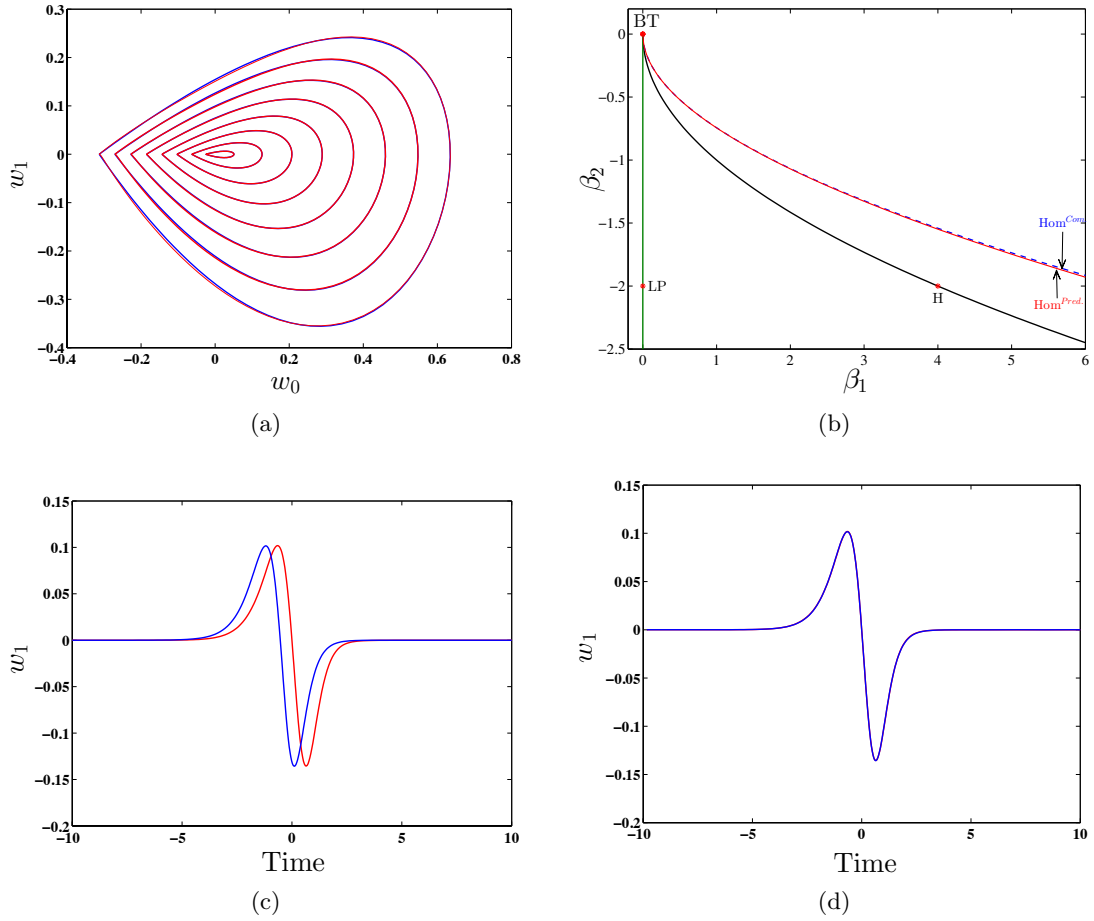

Fig. 2: (a) The comparison of homoclinic orbits in phase space between computed (blue) and predicted (red) using the second-order correction for $\log 10(\beta_1) = -3.921, -3.467, -2.603, -2.094, -1.772, -1.532, -1.342, -1.183, -1.049$. (b) Predicted (red) and computed (dashed blue) homoclinic bifurcation curves in parameter space are hardly distinguishable. The green line is the LP curve. The black curve is the Hopf curve. (c) and (d) The time shift so that the predicted (red) and computed (blue) curves consider at $t = 0$ for $\log 10(\beta_1) = -1.532$.

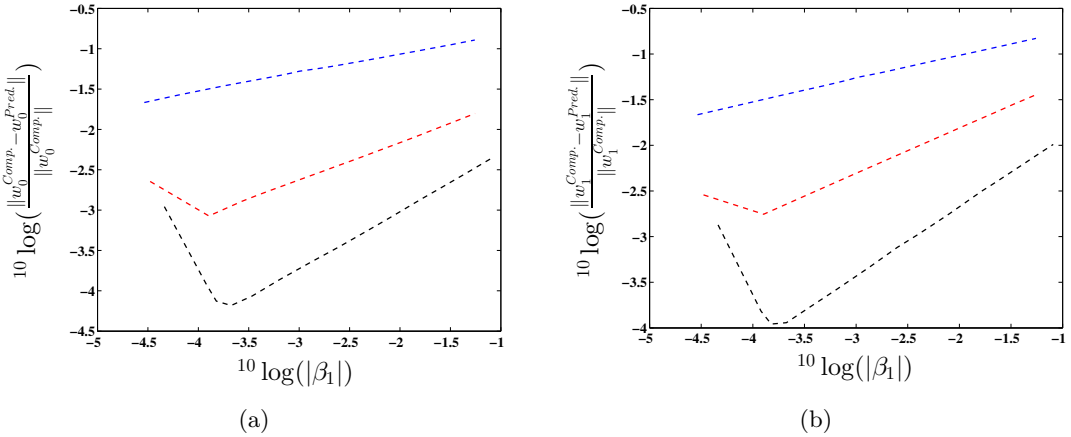

Fig. 3: Accuracy of the predicted w_0 and w_1 functions with Hamiltonian solution (blue), tangent predictor (red) and second-order predictor (black) for $\beta_1 \in [3.85 \times 10^{-5}, 0.05]$. This corresponds to $\varepsilon \in [0.05, 0.35]$. Euclidean norms of the vectors of the function values in the points of the fine mesh are used.

to detect the BT-bifurcation point at $(\beta_1, \beta_2) = (0, 0)$. We start the homoclinic continuation using the BT_Hom initializer, using the predictor (33)-(34) with $\varepsilon = 0.08$. This yields the dashed blue curve Hom^{Com} in Fig. 2a. In Fig. 2b we show the corresponding homoclinic orbits. Observe that the homoclinic orbit is indeed non-symmetric w.r.t. w_0, as is correctly predicted by the improved starter. Next in Fig. 3, we compare the relative errors of the orbit as a function of β_1. The error is computed by taking a computed homoclinic orbit from the numerical continuation. This gives a value of β_1 which yields a value for ε in the predictor. The predictors are then compared with the computed solution using the time points of the fine mesh in the numerical continuation, after a time shift so that the computed and predicted curves coincide for $t = 0$. We see that the improved predictors (red,black) perform better than the one based on the Hamiltonian solution (blue).

5.2. *Indirect field oriented control system*

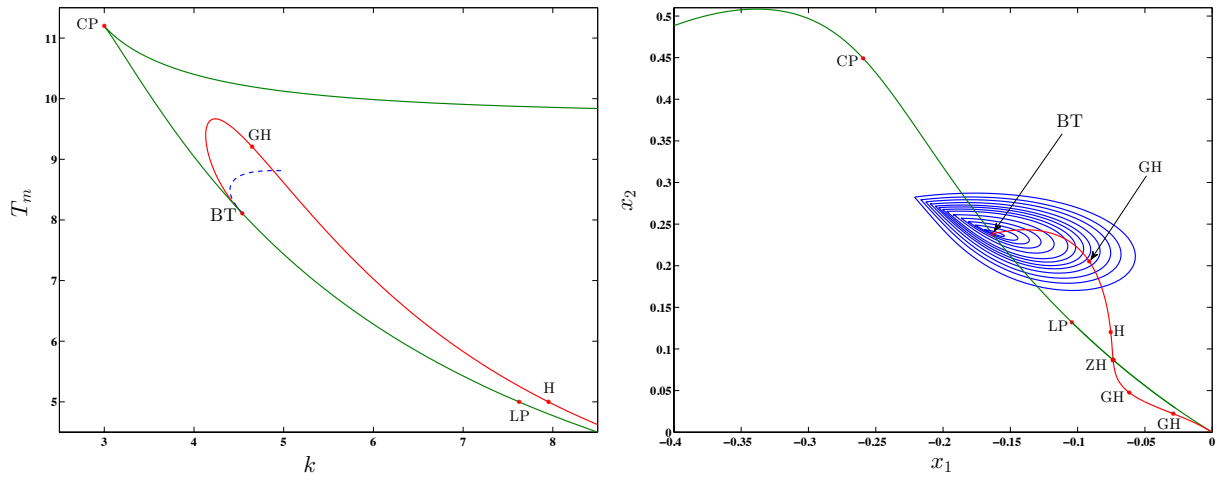

(a) (b)

Fig. 4: (a) Homoclinic orbits emanating from the BT point of the IFOC model in parameter space (k, T_m). The dashed blue curve is the homoclinic orbit. The red line is the Hopf curve and the green line is the LP curve. (b) The homoclinic orbits in state space (x_1, x_2). The green line is the LP curve with three codim 2 points. The red line is the Hopf curve with three generalized Hopf bifurcation points (GH) and ZH point.

The indirect field oriented control (IFOC) system of an induction motor can be mathematically described as in [Bazanella & Reginatto, 2000] and [Salas *et al.*, 2008] by the following ODEs:

$$\begin{cases} \dot{x}_1 = -c_1 x_1 + c_2 x_4 - \frac{k c_1}{u_2^0} x_2 x_4, \\ \dot{x}_2 = -c_1 x_2 + c_2 u_2^0 + \frac{k c_1}{u_2^0} x_1 x_4, \\ \dot{x}_3 = -c_3 x_3 - c_4 c_5 \left(x_2 x_4 - u_2^0 x_1\right) \\ \quad + c_4 \left(T_m + \frac{c_3}{c_4} w_{ref}\right), \\ \dot{x}_4 = -(k_i - k_p c_3) x_3 - k_p c_4 c_5 \left(x_2 x_4 - u_2^0 x_1\right) \\ \quad + k_p c_4 \left(T_m + \frac{c_3}{c_4} w_{ref}\right). \end{cases} \tag{37}$$

Here x_1, x_2, x_3 and x_4 are the state variables, where x_1 and x_2 denote direct and quadrature components of the rotor flux; x_3 is the rotor speed error (i.e., the difference between the reference and the real mechanical speeds of the rotor); and x_4 denotes the quadrature axis component of the stator current. We also define the following constants and parameters: u_2^0 is a constant reference for the rotor flux magnitude; c_1 to c_5 are machine parameters; k_p and k_i are the proportional and the integral PI control gains, respectively; w_{ref} is the speed reference; T_m the load torque; k the measure of rotor time constant mismatches. The

occurrence of LP and Hopf in IFOC have been characterized as a result of rotor time constant mismatches (see, for example, [Bazanella & Reginatto, 2002; Gordillo *et al.*, 2002] and [Moiola & Chen, 1996]). The first results on the occurrence of a BT bifurcation in the IFOC model were presented in [Salas *et al.*, 2004]. A detailed analytical study for the codim 2 bifurcations of (37) can be found in [Salas *et al.*, 2008]. In this paper, we shall examine only the homoclinic orbits that emanate from a given BT point. By continuation of equilibria starting with parameters $k = 17$, $T_m = 5$, $c_1 = 4.4868$, $c_2 = 0.3567$, $c_3 = 0$, $c_4 = 9.743$, $c_5 = 1.911$, $u_2^0 = 11.3$, $k_p = 4.5$, $k_i = 500$, $w_{ref} = 0$, and initial point $(x_1, x_2, x_3, x_4) = (-0.21, 0.11, 2.5)$, MatCont detects an LP point and a Hopf point. Further, by continuation of the limit point with (k, T_m) free, three codim 2 points are detected, BT, ZH and CP.

Table 1: Parameter and state values at the bifurcation points in Fig.4.

Label	k	T_m	State variables
BT	04.54	08.12	$(-0.16, 0.24, 0.00, 10.06)$
CP	03.00	11.20	$(-0.26, 0.45, 0.00, 06.52)$
ZH	11.21	03.43	$(-0.07, 0.09, 0.00, 11.12)$

The normal form coefficients for the BT point are $(a, b) = (28.01, -0.91)$. From the BT point we start the continuation of the homoclinic curve, using k and T_m as free system parameters and with initial amplitude value $\varepsilon = 0.008$ (see Fig.4). This shows that our improved predictor works in higher dimensional systems as well.

References

Arnold, V. I. [1983] *Geometrical Methods in the Theory of Ordinary Differential Equations* (Springer-Verlag, New York, Heidelberg, Berlin).

Bazanella, A. S. & Reginatto, R. [2000] "Robustness margins for indirect field oriented control of induction motors," *IEEE Trans. Autom. Contr.* **45**, 1226–1231.

Bazanella, A. S. & Reginatto, R. [2002] "Instabilty mechanisms in indirect field oriented control drives: Theory and experimental results," *IFAC World Congress* (Barcelona, Spain), Vol. 15, Part I.

Beyn, W.-J. [1994] "Numerical analysis of homoclinic orbits emanating from a Takens-Bogdanov point," *IMA J. Numer. Anal.* **14**, 381–410.

Beyn, W.-J., Champneys, A., Doedel, E. J., Govaerts, W., Kuznetsov, Yu. A. & Sandstede, B. [2002] "Numerical Continuation, and Computation of Normal Forms," *Handbook of Dynamical Systems, II*, ed. Fiedler, B. (Elsevier Science, North Holland), pp. 149–219.

Bogdanov, R. I. [1975] "Versal deformations of a singular point on the plane in the case of zero eigenvalues," *Functional Anal. Appl.* **9**, 144–145.

Bogdanov, R. I. [1976a] "Bifurcations of a limit cycle of a certain family of vector fields on the plane," *Proceedings of Petrovskii Seminar, Vol. 2* (Moscow State University, Moscow), pp. 23–35, in Russian (English translation: *Selecta Math. Soviet.* **1**, 1981, 373-388).

Bogdanov, R. I. [1976b] "The versal deformation of a singular point of a vector field on the plane in the case of zero eigenvalues," *Proceedings of Petrovskii Seminar, Vol. 2* (Moscow State University, Moscow), pp. 37–65, in Russian (English translation: *Selecta Math. Soviet.* **1**, 1981, 389-421).

Champneys, A. R., Kuznetsov, Yu. A. & Sandstede, B. [1996] "A numerical toolbox for homoclinic bifurcation analysis," *Internat. J. Bifur. Chaos Appl. Sci. Engrg.* **6**, 867–887.

De Witte, V., Govaerts, W., Kuznetsov, Yu. A. & Friedman, M. [2012] "Interactive initialization and continuation of homoclinic and heteroclinic orbits in MATLAB," *ACM Trans. Math. Software* **38**, Art. 18, 34.

Dhooge, A., Govaerts, W. & Kuznetsov, Yu. A. [2003] "MATCONT: a MATLAB package for numerical bifurcation analysis of ODEs," *ACM Trans. Math. Software* **29**, 141–164.

Dhooge, A., Govaerts, W., Kuznetsov, Yu. A., Meijer, H. G. E. & Sautois, B. [2008] "New features of the

software MatCont for bifurcation analysis of dynamical systems," *Math. Comput. Model. Dyn. Syst.* **14**, 147–175.

Doedel, E. J. & Kernévez, J. P. [1986] "Auto: Software for continuation and bifurcation problems in ordinary differential equations," Applied mathematics report, California Institute of Technology, Pasadena CA, 226 pages.

Gordillo, F., Salas, F., Ortega, R. & Aracil, J. [2002] "Hopf bifurcation in indirect field-oriented control of induction motors," *Automatica* **38**, 829–835.

Govaerts, W. J. F. [2000] *Numerical methods for bifurcations of dynamical equilibria* (SIAM, Philadelphia, PA).

Guckenheimer, J. & Holmes, P. [1983] *Nonlinear Oscillations, Dynamical Systems and Bifurcations of Vector Fields* (Springer-Verlag, New York).

Kuznetsov, Yu. A. [2004] *Elements of Applied Bifurcation Theory, 3rd ed.* (Springer-Verlag, New York).

Moiola, J. & Chen, G. [1996] *Hopf Bifurcation Analysis: A Frequency Domain Approach* (World Scientific, Singapore).

Salas, F., Gordillo, F. & Aracil, J. [2008] "Codimension-two bifurcations in indirect field oriented control of induction motor drives," *Internat. J. Bifur. Chaos* **18**, 779–792.

Salas, F., Reginatto, R., Gordillo, F. & Aracil, J. [2004] "Bogdanov-Takens bifurcation in indirect field oriented control of induction motor drives," *Proc. CDC* (Atlantis, Bahamas), pp. 4357–4362.

Takens, F. [1974] "Forced oscillations and bifurcations," *Comm. Math. Inst., Rijksuniversiteit Utrecht* **2**, 1–111, reprinted in *Global Analysis of Dynamical Systems*, Instute of Physics, Bristol, 2001, pp. 1–61.